

Article

Electrode Kinetics of Ion Jelly and Ion Sol-Gel Redox Materials on Screen-Printed Electrodes

Rui N. L. Carvalho¹, Cristina M. Cordas^{2,*}  and Luís J. P. da Fonseca^{1,*} 

¹ iBB—Institute for Bioengineering and Biosciences, Instituto Superior Técnico, Universidade de Lisboa, Av. Rovisco Pais, 1049-001 Lisboa, Portugal; ruicarlov@gmail.com

² LAQV, REQUIMTE, Faculdade de Ciências e Tecnologia, Universidade Nova de Lisboa, 2829-516 Caparica, Portugal

* Correspondence: c.cordas@fct.unl.pt (C.M.C.); luis.fonseca@tecnico.ulisboa.pt (L.J.P.d.F.)

Abstract: Several hydrogel materials have been proposed for drug delivery systems and other purposes as interfacial materials, such as components for fuel cells and immobilization of biomolecules. In the present work, two materials, an ion sol-gel, based on 1-octyl-3-methylimidazolium bis(trifluoromethylsulfonyl)imide, and an ion jelly (1-ethyl-3-methylimidazolium ethylsulfate) film deposited on carbon screen-printed electrodes, were electrochemically characterized. The electrode kinetics of ion jelly and ion sol-gel materials were compared by using ferrocyanide/ferricyanide redox reaction couple as a model redox process. Diffusion coefficients were calculated and compared to those obtained with the model redox couple in non-modified electrodes. Results pointed to a decrease of two and four orders of magnitude in the diffusion coefficients, respectively, for ion jelly and ion sol-gel film modified electrodes. Heterogeneous electron transfer constants for the ferrocyanide/ferricyanide ion redox process were also determined for modified and non-modified electrodes, in which the ion sol-gel film modified electrode presented the lower values. This work sought to contribute to the understanding of these materials' properties, with emphasis on their diffusion, conductivity, and electrochemical behavior, namely reversibility, transfer coefficients, and kinetics, and optimize the most suitable properties for different possible applications, such as drug delivery.

Keywords: hydrogel; redox materials; electrochemistry; diffusion coefficients



Citation: Carvalho, R.N.L.; Cordas, C.M.; da Fonseca, L.J.P. Electrode Kinetics of Ion Jelly and Ion Sol-Gel Redox Materials on Screen-Printed Electrodes. *Appl. Sci.* **2022**, *12*, 2087. <https://doi.org/10.3390/app12042087>

Academic Editors: Francisco Jesus Fernandez-Morales and Agnese Magnani

Received: 18 January 2022

Accepted: 15 February 2022

Published: 17 February 2022

Publisher's Note: MDPI stays neutral with regard to jurisdictional claims in published maps and institutional affiliations.



Copyright: © 2022 by the authors. Licensee MDPI, Basel, Switzerland. This article is an open access article distributed under the terms and conditions of the Creative Commons Attribution (CC BY) license (<https://creativecommons.org/licenses/by/4.0/>).

1. Introduction

Hybrid materials have attracted much interest in research aiming for novel materials and applications. Among these are the so-called 'ionogels' that consist of an ionic liquid (IL) immobilized in a solid/gel matrix. Part of their attractiveness is that they possess the conductive properties of ILs and the physical properties of the matrix materials used, and the physicochemical properties can be tuned by choosing from an enormous array of cation–anion pairs. The ionogels described in the literature continue to grow in number and have been the subjects of various reviews [1–4]. One of the most common approaches is to use polymers to entrap or chemically bind the IL. These IL-infused gels have been explored for various fields of application, from drug delivery agents to catalysts, sensors, and electrolyte membranes [5–7]. An effort is being made to replace conventional media, solvents, and materials in batteries with IL-based materials, mainly as electrolytes or electrode materials [8]. Likewise, studies on ionogels applied to fuel cells have shown they could be used as proton-exchange membranes on H₂/O₂ fuel cells [9,10] and that protic ionogels could result in highly conductive electrolytes with favorable properties [11]. Ionogels have also been studied as catalytic membranes by loading the material with various types of catalysts. Since some ILs work well in enhancing the activity and stability of enzymes [12,13], some ionogels are an attractive medium for biocatalysis, namely for building electrodes for enzymatic fuel cells or as biosensors [14–16].

Ion jelly (IJ) is a macromolecular gel material that uses gelatin as the solid phase and is obtained by mixing water and hydrophilic ionic liquids [17]. Ionic and hydrogen bonds are established, creating a microenvironment appropriate for biomolecule immobilization and stabilization, with cytochrome *c* and some oxidoreductases having been used as model enzymes for immobilization in IJ [15,18,19]. Being gelatin-based, IJ can be easily molded into various shapes, such as membranes or fibers [20,21]. The IL employed dictates the maximum conductivity of the material. Experiments with 1-butyl-3-methylimidazolium dicyanamide ([BMIM][DCA]) containing IJ showed that at a high IL/gelatin ratio (3:1 *w/w*), the density of charge carriers per volume is comparable to that of a pure IL, meaning that the ionic conductivity of IJ and ILs were about the same, reaching 10^{-2} S/cm [22,23]. However, studies of the swelling kinetics of IJ in water showed extensive leakage of ionic liquid from the matrix, limiting its applicability [24]. More recently, novel materials based on different types of natural biopolymers and ILs have arisen, combining, for instance, 1-ethyl-3-methylimidazolium acetate ([EMIm][OAc]) or cholinium lysinate ([Ch][Lys]) and cellulose to yield new membrane materials with high porosity and conductivity [25,26].

Colloidal ionic liquid gels based on silica structures have also garnered much interest [1,27]. The most common method to obtain these structures is through the use of alkoxysilanes in the presence of an IL, water, alcohol, and a catalyst, forming a final material suitable for immobilizing biomolecules, depending on the IL used [28–31]. Tetramethyl orthosilicate (TMOS) and tetraethyl orthosilicate (TEOS) are some of the most commonly used precursors [32], but other derivatives also have been used [30,33]. A different method of obtaining a silica sol-gel consists of a two-component non-hydrolytic process involving formic acid and an alkoxysilane [34]. Vioux and co-workers created a particularly interesting family of ionic liquid sol-gels (also named ionogels by their authors), that was obtained by confining 1-butyl-3-methylimidazolium bis(trifluoromethylsulfonyl)imide ([bmim][TFSI]) in a silica sol-gel through the formic acid method [35]. If only TMOS was used, the resulting IL was easily removed from the ionogel when immersed in water, but by employing equimolar amounts of TMOS and methyltrimethyl orthosilicate (MTMS) instead of TMOS alone, the ionogel became completely water-stable [36]. However, in another work, it was observed that only when using ([omim][TFSI]) was the ionic liquid leakage almost nonexistent, with ([bmim][TFSI]) gels still experiencing some washout in water [37].

Drug delivery systems are characterized by a burst or prolonged release of the target drug, especially after swelling in contact with human fluids, with toxic or inefficient consequences for the patient's health [38]. Today, drug loading capacity in delivery systems, drug targeting, and precise control of the drug release in the required conditions, is a crucial factor in developing a reliable drug delivery system [39,40]. For that reason, the design of new biocompatible and tailor-made carrying matrixes, their characterization and evaluation of their diffusion properties, particularly in swelling conditions, are of fundamental importance [41]. Physical and chemical methodologies including new ones such as electrochemical characterization can contribute to a better understanding of the new tailor-made carrying matrixes' behavior and facilitate the design of more efficient drug delivery systems (DDS) [42]. Electrochemistry methods can contribute not only to the materials' characterization but also to the development of diffusion-controlled DDS based on in-situ potential or current imposition [43].

In the current work, the electrode kinetics of IJ and a silica-based ionogel (ISG) were compared using cyclic voltammetry and the ferrocyanide/ferricyanide pair used as a probe. This redox couple is a frequently used model for testing several materials and aqueous systems [44]. It has been used to study microfabricated iridium electrodes [45] and single-walled carbon nanotubes [46] among many other systems and has also been used previously in IJ materials [18]. In addition to comparing the IJ and silica-based ionogel properties, namely diffusion coefficients and electrochemical behavior such as conductivity, reversibility, transfer coefficients, and kinetics, it was possible to assess the materials' viability for future development applications, namely drug-delivery.

2. Materials and Methods

2.1. Preparation of IJ and ISG

1-Ethyl-3-methylimidazolium ethylsulfate ([emim][EtSO₄]) was supplied by Strem Chemicals (Newburyport, MA, USA). 1-octyl-3-methylimidazolium bis(trifluoromethylsulfonyl)imide ([omim][TFSI]) and 1-butyl-3-methylimidazolium bis(trifluoromethylsulfonyl)imide ([bmim][TFSI]) were purchased from IoLiTec (Heilbronn, Germany). Bacteriological gelatin, type A “Cultimed”, was purchased from Panreac (Castellar del Vallès, Spain). All other chemicals mentioned were purchased from Sigma-Aldrich (St. Louis, MO, USA). Solutions for electrochemical measurements were prepared with deionized water from a Milli-Q water purification system, while the rest used double distilled (dH₂O) water.

Screen-printed electrodes (DRP 110) were acquired from Metrohm Dropsens (Asturias, Spain): both secondary and working electrode materials were carbon ink, and the pseudo-reference electrode was made of silver ink.

The IJ preparation method was based on a previously described protocol [47]. IJ films were prepared by mixing $100 \times 10^{-6} \text{ dm}^3$ ([emim][EtSO₄]) with 0.040 g of gelatin and $260 \times 10^{-6} \text{ dm}^3$ of $0.02 \text{ mol} \cdot \text{dm}^{-3}$ Tris-HCl buffer, pH 7.5 at 60 °C, until reaching homogeneity (typically within a few minutes). After 5 min of further stirring, $50 \times 10^{-6} \text{ dm}^3$ aliquots of each solution were deposited on the carbon SPEs. The deposited solution was then left to gel for 1 h at room temperature, followed by maturation under controlled humidity for 4 days inside the headspace of a closed chamber containing a saturated aqueous solution of sodium chloride (water activity, *a_w* of 0.76 [48]). After 4 days in these conditions, the IJ's weight reached equilibrium and was considered mature and ready for use. When depositing on SPEs, the gel was made to cover the three-electrode system (Figure 1).

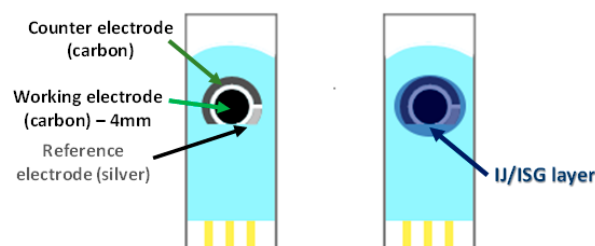


Figure 1. Representation of a clean SPE (left), and an SPE covered with a layer of IJ or ISG on top (right).

Ion sol-gel (ISG) was prepared by using a sol-gel route for immobilizing ionic liquids in silica matrixes using alkoxy silanes (AS) [35,37]. TMOS and MTMS were added to a solution of ([omim][TFSI]) or ([bmim][TFSI]) in formic acid, in a molar ratio of 0.5:0.5:7.8:1 (TMOS:MTMS:FA:IL). A 15% vol of 50 mM sodium PB buffer pH 7.6 and 4% of ([omim][BF₄]) were added, and after a very brief stirring, $75 \times 10^{-6} \text{ dm}^3$ of solution was deposited (also covering all three electrodes as done on SPEs). Maturation occurred at room conditions for 7 days.

The swelling was carried out in conditions similar to those in previous work [24]. Matured films were weighted accurately and placed inside sample container flask caps, then immersed in $7 \times 10^{-3} \text{ dm}^3$ of distilled water at 4 °C. The swelling was carried out until a visible equilibrium was reached (24 h). Post-swelling films were removed from excess water and underwent a repetition of the maturation process.

2.2. Electrochemical and Conductivity Measurements

Cyclic voltammetry (CV) assays of IJ or ISG modified SPEs were carried out in the same anaerobic conditions as described in previous work performed with ion jelly [15] inside an anaerobic chamber (O₂ conc. < 0.1 ppm) (MBraun Unilab–Oststeinbek, Germany). SPEs and all the solutions were degassed under a flow of argon in anaerobic flasks prior to use and inserted in the anaerobic chamber. CV assays were performed using a AUTOLAB type III potentiostat. The working, counter, and pseudo-reference electrodes of the SPEs

were carbon, carbon, and silver ink, respectively; $0.1 \text{ mol}\cdot\text{dm}^{-3} \text{ KNO}_3/0.02 \text{ mol}\cdot\text{dm}^{-3}$ Tris-HCl buffer, pH 7.5, was used as supporting electrolyte. The diffusive properties of TMOS/MTMS ion sol-gel were analyzed electrochemically and compared to those of IJ. Three configurations were compared: (1) clean SPEs (no deposited material); (2) SPEs containing a single layer of [emim][EtSO₄]-IJ (SPE-IJ); (3) SPEs with a single layer of [omim][TFSI]-ISG (ion sol-gel, SPE-ISG).

The conductivity of IJ and ISG was determined by dielectric relaxation spectroscopy. Films with 20 mm of diameter and thickness ranging from 0.8 to 1.1 mm were placed between two gold electrodes (the smaller electrode had a 10 mm diameter) in a parallel plate capacitor, BDS 1200. Measurements were carried out with an Alpha-N analyzer from Novocontrol GmbH, using a frequency range from 10^{-1} to 106 Hz.

CV experiments aiming to determine the diffusive properties of the studied materials were carried out in room temperature conditions using a CHI Instruments 440B Electrochemical Analyzer (Austin, TX, USA), with the samples placed inside a Faraday cage. A $30 \times 10^{-6} \text{ dm}^3$ drop of a solution of $10 \times 10^{-3} \text{ mol}\cdot\text{dm}^{-3} \text{ K}_3\text{Fe}(\text{CN})_6$ in $1 \text{ mol}\cdot\text{dm}^{-3} \text{ KNO}_3$ was added on top of the SPEs, and scans were initiated after a 5 min resting period. CV runs were for 3 cycles and the scan rates used were 2.5, 5, 10, 50, 100 and $200 \text{ mV}\cdot\text{s}^{-1}$. To calculate the diffusion coefficient of the oxidized (D_{O}) and reduced species (D_{R}), the Randles–Sevcik equation [49] was applied. Details on the method are given as supplementary information.

3. Results and Discussion

3.1. Conductivity Characterization of Ion Jelly and Ion Sol-Gel

ISG was previously demonstrated to be stable in water, and while the native conductivity of ISG films is one to two orders of magnitude lower than that of IJ, the opposite happens in swollen films, with conductivity of [omim][TFSI] ISG surpassing that of IJ by one to two orders of magnitude (Figure 2).

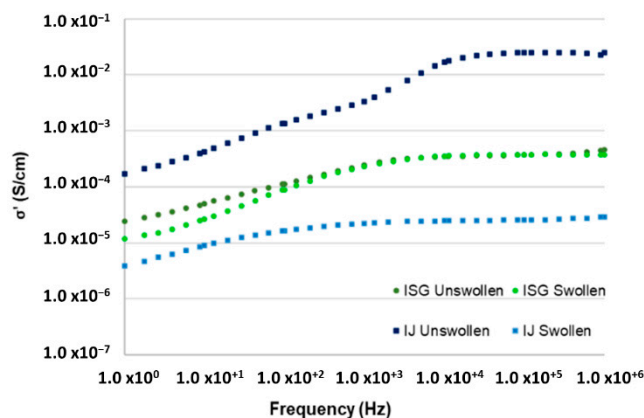


Figure 2. Real part of conductivity for ISG with [omim][TFSI], and IJ made with [emim][EtSO₄], at 20 °C.

The spectra of IJ were in accordance with previous studies, exhibiting a plateau in the high-frequency region, but no plateau in the low-frequency region, a trait shared by the pristine ionic liquid on which IJ was based [50]. ISG shared a similar type of spectra, and was likewise close in conductivity to pristine [omim][TFSI] [51].

3.2. Electrochemical Characterization of IJ and ISG

In order to compare the electrochemical properties of each material, the redox couple ferricyanide/ferrocyanide was chosen for being one of the most well-studied reversible single-step electron transfer processes, providing well-defined peaks, thus being a good redox model for diffusion studies [44]. Voltammogram characteristics of $\text{Fe}(\text{CN})_6^{3-}/\text{Fe}(\text{CN})_6^{4-}$ redox behavior on a clean SPE, a modified SPE covered with an IJ

film (SPE-IJ), and a modified SPE with an ISG film (SPE-ISG) are represented in Figure 3. The formal potentials, peak separations and peak symmetries are shown in Table 1.

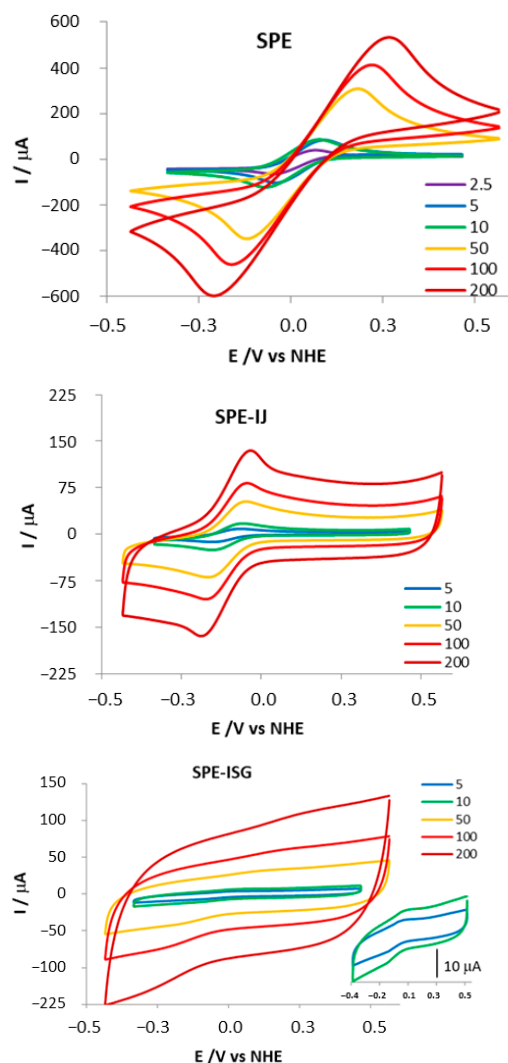


Figure 3. Representative 3rd cycles of the cyclic voltammograms attained with $10 \times 10^{-3} \text{ mol}\cdot\text{dm}^{-3}$ $\text{Fe}(\text{CN})_6^{3-}/\text{Fe}(\text{CN})_6^{4-}$ in $1 \text{ mol}\cdot\text{dm}^{-3}$ KNO_3 at various scan rates for SPE, SPE-IJ and SPE-ISG (inset is a magnification of the lower scan rates, in $\text{mV}\cdot\text{s}^{-1}$), respectively.

The peak separations of $\text{Fe}(\text{CN})_6^{3-}/\text{Fe}(\text{CN})_6^{4-}$ pair on clean SPEs were affected by the scan rate used, with large values of ΔE_p being observed at scan rates above $50 \text{ mV}\cdot\text{s}^{-1}$, which is in agreement with the less reversible behavior at higher scan rates. The formal potential of the process was on average $+157 \pm 10 \text{ mV}$. Anodic and cathodic peak symmetry (ratio I_{pc}/I_{pa}) were also not affected by the scan rate, as expected for a reversible process, with values close to 1 on all tested scan rates. $|E_p - E_p/2|$ was approximately constant at 80 mV for scan rates up to $10 \text{ mV}\cdot\text{s}^{-1}$, rising up to 185 mV at higher scan rates. Observation of the typical reversible behavior of the ferricyanide redox pair process is often dependent on pretreatment of the electrode surfaces [45]. At high scan rates, large peak separations are commonly observed on many surfaces, falling into quasi-reversible behavior [46,52]. A difference of 56 mV in $|E_p - E_p/2|$, as well as a ΔE_p of 57 mV, which are characteristic of ideal reversible processes, are rarely found in experimental conditions. This potential difference is due to several factors, such as solution resistance [53] and also incomplete removal/depletion of reduced or oxidized species at the switching potentials. Faradaic current would have to decay completely to zero before the reverse scan was initiated

in order to minimize this factor, which is not very practical, as it involves stopping the measurement and holding it at very negative potentials [54]. Therefore, even experimental ΔE_p values for one-electron reversible systems with fast kinetics are usually 70 mV or greater [55]. Taking all of this into consideration, the behavior of ferrocyanide in carbon SPEs appeared to be reversible in the low scan rate region but exhibited a quasi-reversible behavior in the high scan rate region.

Table 1. Formal reduction potentials, peak separation and ratio of the anodic and cathodic current peaks as a function of scan rate for the $\text{Fe}(\text{CN})_6^{3-}/\text{Fe}(\text{CN})_6^{4-}$ redox couple in SPE, SPE-IJ and SPE-ISG. Values are averages of the data obtained from all 3 cycles, and respective standard deviation.

ν ($\text{mV}\cdot\text{s}^{-1}$)		2.5	5	10	50	100	200
SPE	$E^{\circ'}$ (mV)	145 ± 5	159 ± 4	141 ± 2	166 ± 1	165 ± 1	162 ± 3
	ΔE_p (mV)	113 ± 2	130 ± 1	147 ± 2	302 ± 1	381 ± 2	477 ± 4
	I_{pc}/I_{pa}	1.05 ± 0.03	1.01 ± 0.01	1.02 ± 0.01	1.00 ± 0.01	1.03 ± 0.02	1.07 ± 0.05
SPE-IJ	$E^{\circ'}$ (mV)		24 ± 2	28 ± 1	26 ± 1	25 ± 1	23 ± 2
	ΔE_p (mV)	-	90 ± 1	95 ± 3	120 ± 1	129 ± 1	155 ± 1
	I_{pc}/I_{pa}		1.14 ± 0.02	1.24 ± 0.02	1.15 ± 0.01	1.16 ± 0.01	1.17 ± 0.02
SPE-ISG	$E^{\circ'}$ (mV)		103 ± 1	98 ± 1	100 ± 2	113 ± 9	117 ± 5
	ΔE_p (mV)	-	103 ± 1	113 ± 2	256 ± 6	412 ± 5	542 ± 10
	I_{pc}/I_{pa}		0.40 ± 0.01	0.41 ± 0.04	0.95 ± 0.13	1.37 ± 18	1.15 ± 0.25

Due to the changes ion jelly undergoes when it comes in contact with aqueous solutions, scan rates that involve a long running time ($2.5 \text{ mV}\cdot\text{s}^{-1}$) were not performed, and CV assays were performed for only two cycles in order to minimize the experimental time. The formal potential of $\text{Fe}(\text{CN})_6^{3-}/\text{Fe}(\text{CN})_6^{4-}$ in SPE-IJ electrodes was on average $+26 \pm 1 \text{ mV}$, a shift of about 130 mV in the negative direction when compared with the unmodified electrodes (Figure 3). Maximum peak currents were considerably inferior in the presence of IJ, which was expected since having a gel matrix on top of an electrode hinders molecule diffusion. Peak symmetry was lower, with an average I_{pc}/I_{pa} of 1.17.

Peak intensity in the ion sol-gel (ISG) system was markedly lower, which was indicative of severely hindered diffusion (Figure 3). A larger baseline hysteresis was observed, which corresponded to high capacitive currents. The formal potentials of the reaction fell in between those observed in SPE and SPE-IJ, at $+106 \pm 7 \text{ mV}$. Variation of peak separation with scan rate followed a profile similar to that of the unmodified SPE: at lower scan rates variation was small, but above $50 \text{ mV}\cdot\text{s}^{-1}$ it rose sharply, up to 542 mV. Unlike the other two cases, the I_{pc}/I_{pa} ratio in ion sol-gel oscillated between 0.4 at low scan rates and 1.3 at high scan rates. Irreversible behavior was initially considered based on this atypical behavior and high peak separations. Diffusion coefficients for each system were calculated from the slopes of peak current against the square root of the scan rate (Figure 4). The Randles–Sevcik equation was used to calculate D_O and D_R in unmodified SPE and in ion jelly-modified SPE, while the modified equation for irreversible processes [55] was used for ISG-modified electrodes. The results are summarized in Table 2. The value of α used was obtained according to a reported method [56]; α for the scan rates where kinetics were more irreversible, corresponding to the $\Delta E_p \geq 300 \text{ mV}$ ($\nu = 50, 100$ and $200 \text{ mV}\cdot\text{s}^{-1}$) were used. Those charge transfer coefficients were averaged out, giving a mean $\alpha = 0.56$.

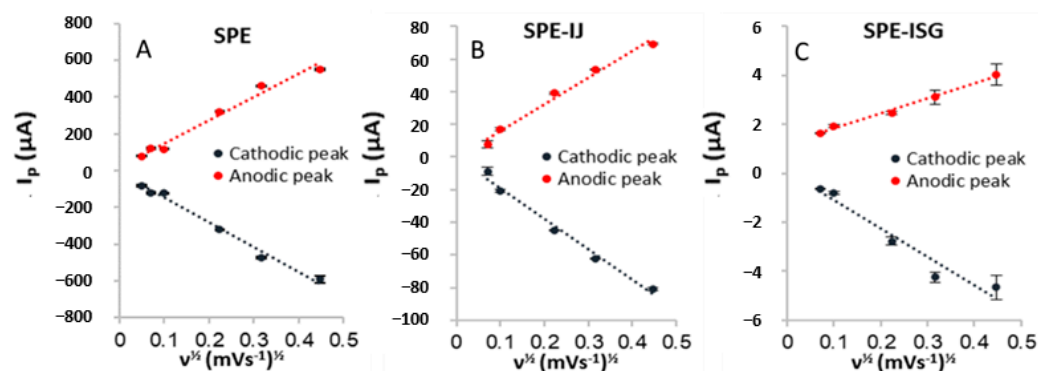


Figure 4. Anodic and cathodic peak currents as a function of the square root of the scan rate. Values are averages from the three cycles and error bars are the standard deviation: (A) SPE, (B) IJ-modified SPE and (C) ISG-modified SPE.

Table 2. Diffusion coefficients and electron transfer rate constants for the three electrode types used. Values are averages of all cycles and errors are the standard deviation.

Electrode Type	D_O ($\text{cm}^2 \cdot \text{s}^{-1}$)	D_R ($\text{cm}^2 \cdot \text{s}^{-1}$)	k^0 ($\text{cm} \cdot \text{s}^{-1}$)
SPE	$(1.57 \pm 0.14) \times 10^{-5}$	$(1.38 \pm 0.01) \times 10^{-5}$	$(1.03 \pm 0.03) \times 10^{-3}$
SPE-IJ	$(3.07 \pm 0.56) \times 10^{-7}$	$(2.29 \pm 0.62) \times 10^{-7}$	$(1.54 \pm 0.38) \times 10^{-2}$
SPE-ISG	$(1.73 \pm 0.35) \times 10^{-9}$	$(4.79 \pm 1.37) \times 10^{-10}$	$(7.53 \pm 0.11) \times 10^{-6}$

As expected, diffusion coefficients were lower when a layer of material covered the electrode, as it imposes a physical barrier to the diffusion of molecules to and from the electrode's surface. The diffusion coefficients were very close for $\text{Fe}(\text{CN})_6^{3-}$ and $\text{Fe}(\text{CN})_6^{4-}$, since both ions have approximately the same size, an octahedral structure, and behave similarly in solvated environments [46]. However, in the ion sol-gel matrix, diffusion of $\text{Fe}(\text{CN})_6^{4-}$ was significantly lower than that of its oxidized form. D_O and D_R were two orders of magnitude lower in IJ-modified electrode than in an unmodified SPE, resembling the diffusion coefficients of water obtained in the swelling experiments of ion jelly [24].

In ISG, D_O and D_R were a whole four to five orders of magnitude lower than in the SPEs, which is in agreement with the very low peak currents measured. However, considering that other silica-based ionogels have shown much greater responses by cyclic voltammetry [28], the cause for this hindered diffusion most likely lies in the methylation of the silica network that allows the retention of [omim][TFSI] during water immersion. A possible solution to this problem that at the same time avoids sacrificing water stability could lie in a different method of immobilizing an alkylimidazole TFSI IL, which was investigated by Opallo and co-workers [57]. They covalently bonded the IL to a TMOS silica network by using an alkylimidazolium cation with an alkoxide group, which participated in the creation of the silicate matrix. Kinetic studies using ferrocyanide in a tin oxide electrode with this sol-gel showed intense peak currents and a voltammogram typical of a reversible process [57,58]. Regarding the determination of k^0 , SPE-IJ had $\Delta E_p < 200$ mV for all scan rates tested, so Nicholson's method was enough to calculate the kinetic parameter Ψ . Both SPE-ISG and SPE had peak separations outside Nicholson's working curve (Figure 5), so the suitable equations were used to cover the whole range of scan rates [59].

From the slopes of $\Psi-v^{-1/2}$ plots [59], values for k^0 were obtained for each of the electrode types (Table 2). The charge transfer coefficient for electrodes featuring reversible and quasi-reversible behavior (SPE and SPE-IJ) was considered 0.5, in accordance with the criteria of Nicholson's working curve and some α values found in the literature for the $\text{Fe}(\text{CN})_6^{3-}/\text{Fe}(\text{CN})_6^{4-}$ redox pair [60]. With k^0 in the order of 10^{-3} and 10^{-2} $\text{cm} \cdot \text{s}^{-1}$, the redox reactions in the SPE and SPE-IJ fell into quasi-reversible kinetics, with the process that occurs with ion jelly being closer to the reversibility limit, which was in agreement with the initial observations of cyclic voltammograms. In SPE-ISG, the k^0 of 10^{-6} $\text{cm} \cdot \text{s}^{-1}$ fell

squarely within the irreversible region, validating the initial assumption made. Although the ISG material was found to have a lower diffusion and rate transfer constant when compared with IJ and other materials, that was not a deterrent to its use in real applications, such as drug delivery.

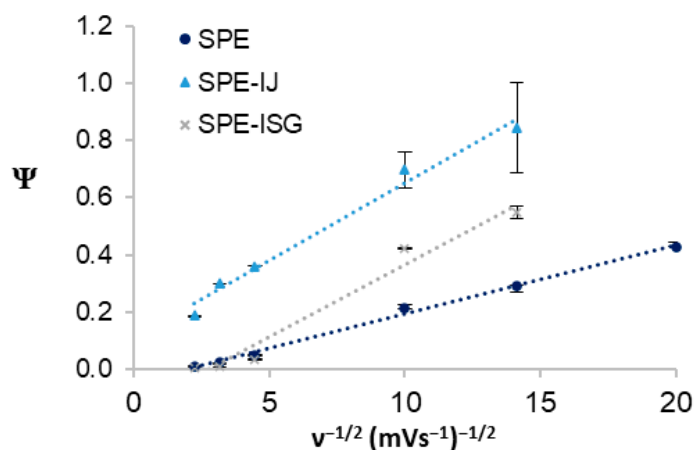


Figure 5. Plot of the kinetic parameter Ψ as a function of $\nu^{-1/2}$ for the three electrode types used.

4. Conclusions

Diffusion constants and electron transfer rate constants were determined for the ferricyanide/ferrocyanide pair in IJ- and ISG-modified electrodes. Molecule diffusion was found to be much more hindered in ISG than in IJ, resulting in the observation of poorly defined redox peaks of $\text{Fe}(\text{CN})_6^{3-}/\text{Fe}(\text{CN})_6^{4-}$. While this means the current ion sol-gel is not ideal for applications that require solute diffusion, the fact that it is stable in water and does not leak out IL, retaining reasonable conductivities throughout, could prove interesting for other applications that need water-resistant conductive membranes, such as drug delivery. In fact, ISG biocompatible materials can provide more stability and higher control of the drug release, in a time scale that many other biomaterials may not [61]. For instance liposome systems for drug delivery still present several unresolved problems, such as attacks from the immune system via opsonization by proteins [62].

Author Contributions: Conceptualization, C.M.C. and L.J.P.d.F.; Formal analysis, R.N.L.C. and C.M.C.; Investigation, R.N.L.C.; Methodology, C.M.C.; Supervision, L.J.P.d.F.; Validation, L.J.P.d.F.; Writing—original draft, R.N.L.C.; Writing—review & editing, C.M.C. and L.J.P.d.F. All authors have read and agreed to the published version of the manuscript.

Funding: FCT—Fundação para a Ciência e a Tecnologia, Portugal (R. N. L. C awarded with grant number SFRH/BD/77568/2011). This work was supported by the Associate Laboratory for Green Chemistry—LAQV which is financed by national funds from FCT/MCTES (UIDB/50006/2020). Authors also acknowledge iBB—Institute for Bioengineering and Biosciences for funding through project UIDB/04565/2020.

Institutional Review Board Statement: Not applicable.

Informed Consent Statement: Not applicable.

Data Availability Statement: Raw data available on request.

Conflicts of Interest: The authors declare no conflict of interest.

References

- Vioux, A.; Viau, L.; Volland, S.; Le Bideau, J. Use of ionic liquids in sol-gel; ionogels and applications. *C. R. Chim.* **2010**, *13*, 242–255. [[CrossRef](#)]
- Le Bideau, J.; Viau, L.; Vioux, A. Ionogels, ionic liquid based hybrid materials. *Chem. Soc. Rev.* **2010**, *40*, 907–925. [[CrossRef](#)]

3. Marr, P.C.; Marr, A.C. Ionic liquid gel materials: Applications in green and sustainable chemistry. *Green Chem.* **2015**, *18*, 105–128. [[CrossRef](#)]
4. Tiago, G.A.O.; Matias, I.A.S.; Ribeiro, A.P.C.; Martins, L.M.D.R.S. Application of Ionic Liquids in Electrochemistry—Recent Advances. *Molecules* **2020**, *25*, 5812. [[CrossRef](#)]
5. Viau, L.; Tourné-Péteilh, C.; Devoisselle, J.-M.; Vioux, A. Ionogels as drug delivery system: One-step sol–gel synthesis using imidazolium ibuprofenate ionic liquid. *Chem. Commun.* **2009**, *46*, 228–230. [[CrossRef](#)] [[PubMed](#)]
6. Pedro, S.; Freire, C.; Silvestre, A.; Freire, M. Ionic Liquids in Drug Delivery. *Encyclopedia* **2021**, *1*, 27. [[CrossRef](#)]
7. Gao, Y.-R.; Cao, J.-F.; Shu, Y.; Wang, J.-H. Research progress of ionic liquids-based gels in energy storage, sensors and antibacterial. *Green Chem. Eng.* **2021**, *2*, 368–383. [[CrossRef](#)]
8. Yang, Q.; Zhang, Z.; Sun, X.-G.; Hu, Y.-S.; Xing, H.; Dai, S. Ionic liquids and derived materials for lithium and sodium batteries. *Chem. Soc. Rev.* **2018**, *47*, 2020–2064. [[CrossRef](#)] [[PubMed](#)]
9. Lakshminarayana, G.; Nogami, M. Inorganic–organic hybrid membranes with anhydrous proton conduction prepared from tetramethoxysilane/methyl-trimethoxysilane/trimethylphosphate and 1-ethyl-3-methylimidazolium-bis (trifluoromethanesulfonyl) imide for H₂/O₂ fuel cells. *Electrochim. Acta* **2010**, *55*, 1160–1168. [[CrossRef](#)]
10. Chang, W.-Q.; Apodaca, D.C.; Peng, W.-C.; Chen-Yang, Y.-W. Protic ionic liquid-containing silica-based ionogels for nonhumidified PEMFC applications. *Ionics* **2017**, *24*, 469–481. [[CrossRef](#)]
11. Yasuda, T.; Watanabe, M. Protic ionic liquids: Fuel cell applications. *MRS Bull.* **2013**, *38*, 560–566. [[CrossRef](#)]
12. Yan, R.; Zhao, F.; Li, J.; Xiao, F.; Fan, S.; Zeng, B. Direct electrochemistry of horseradish peroxidase in gelatin-hydrophobic ionic liquid gel films. *Electrochim. Acta* **2007**, *52*, 7425–7431. [[CrossRef](#)]
13. Matias, S.C.; Lourenço, N.M.T.; Fonseca, L.J.P.; Cordas, C.M. Comparative Electrochemical Behavior of Cytochrome c on Aqueous Solutions Containing Choline-Based Room Temperature Ionic Liquids. *ChemistrySelect* **2017**, *2*, 8701–8705. [[CrossRef](#)]
14. Sun, L.; Zhang, X.; Wang, W.; Chen, J. Carbon nanotube–ionic liquid composite gel based high-performance bioanode for glucose/O₂ biofuel cells. *Anal. Methods* **2015**, *7*, 5060–5066. [[CrossRef](#)]
15. Carvalho, R.; Almeida, R.M.; Moura, J.J.G.; Lourenço, N.T.; Fonseca, L.J.P.; Cordas, C.M. Sandwich-Type Enzymatic Fuel Cell Based on a New Electro-Conductive Material—Ion Jelly. *ChemistrySelect* **2016**, *1*, 6546–6552. [[CrossRef](#)]
16. Pandey, P.K.; Rawat, K.; Aswal, V.K.; Kohlbrecher, J.; Bohidar, H.B. DNA ionogel: Structure and self-assembly. *Phys. Chem. Chem. Phys.* **2016**, *19*, 804–812. [[CrossRef](#)] [[PubMed](#)]
17. Vidinha, P.; Lourenço, N.M.T.; Pinheiro, C.; Brás, A.R.; Carvalho, T.; Santos-Silva, T.; Mukhopadhyay, A.; Romão, M.J.; Parola, J.; Dionisio, M.; et al. Ion jelly: A tailor-made conducting material for smart electrochemical devices. *Chem. Commun.* **2008**, 5842–5844. [[CrossRef](#)] [[PubMed](#)]
18. Cordas, C.; Lourenço, N.; Vidinha, P.; Afonso, C.; Barreiros, S.; Fonseca, L.P.; Cabral, J.M. New conducting biomaterial based on Ion Jelly® technology for development of a new generation of biosensors. *New Biotechnol.* **2009**, *25*, S138–S139. [[CrossRef](#)]
19. Lourenço, N.M.T.; Österreicher, J.; Cabral, J.M.S.; Fonseca, L.P.; Vidinha, P.; Barreiros, S. Evaluation of Ion Jelly biopolymer on glucose biosensing. In Proceedings of the 1st Portuguese Biomedical Engineering Meeting, Lisbon, Portugal, 1–4 March 2011; pp. 1–4. [[CrossRef](#)]
20. Couto, R.; Neves, L.; Simões, P.; Coelho, I. Supported Ionic Liquid Membranes and Ion-Jelly® Membranes with [BMIM][DCA]: Comparison of Its Performance for CO₂ Separation. *Membranes* **2015**, *5*, 13–21. [[CrossRef](#)] [[PubMed](#)]
21. Dos Santos, R.; Rocha, Á.; Matias, A.; Duarte, C.; Sá-Nogueira, I.; Lourenço, N.; Borges, J.P.; Vidinha, P. Development of antimicrobial Ion Jelly fibers. *RSC Adv.* **2013**, *3*, 24400–24405. [[CrossRef](#)]
22. Carvalho, T.; Augusto, V.; Brás, A.R.; Lourenço, N.M.T.; Afonso, C.A.M.; Barreiros, S.; Correia, N.T.; Vidinha, P.; Cabrita, E.J.; Dias, C.J.; et al. Understanding the Ion Jelly Conductivity Mechanism. *J. Phys. Chem. B* **2012**, *116*, 2664–2676. [[CrossRef](#)] [[PubMed](#)]
23. Carvalho, T.; Augusto, V.; Rocha, A.; Lourenço, N.M.T.; Correia, N.T.; Barreiros, S.; Vidinha, P.; Cabrita, E.J.; Dionísio, M. Ion Jelly Conductive Properties Using Dicyanamide-Based Ionic Liquids. *J. Phys. Chem. B* **2014**, *118*, 9445–9459. [[CrossRef](#)] [[PubMed](#)]
24. De Carvalho, R.N.L.; Lourenço, N.M.T.; Gomes, P.M.V.; da Fonseca, L.J.P. Swelling behavior of gelatin-ionic liquid functional polymers. *J. Polym. Sci. Part B Polym. Phys.* **2013**, *51*, 817–825. [[CrossRef](#)]
25. Nevstrueva, D.; Murashko, K.; Vunder, V.; Aabloo, A.; Pihlajamäki, A.; Mänttari, M.; Pyrhönen, J.; Koironen, T.; Torop, J. Natural cellulose ionogels for soft artificial muscles. *Colloids Surf. B Biointerfaces* **2018**, *161*, 244–251. [[CrossRef](#)]
26. Villar-Chavero, M.M.; Domínguez, J.C.; Alonso, M.V.; Rigual, V.; Oliet, M.; Rodriguez, F. Viscoelastic properties of physical cellulosic ionogels of cholinium lysinate. *Int. J. Biol. Macromol.* **2019**, *133*, 262–269. [[CrossRef](#)] [[PubMed](#)]
27. Ueno, K.; Hata, K.; Katakabe, T.; Kondoh, M.; Watanabe, M. Nanocomposite Ion Gels Based on Silica Nanoparticles and an Ionic Liquid: Ionic Transport, Viscoelastic Properties, and Microstructure. *J. Phys. Chem. B* **2008**, *112*, 9013–9019. [[CrossRef](#)] [[PubMed](#)]
28. Liu, Y.; Shi, L.; Wang, M.; Li, Z.; Liu, H.; Li, J. A novel room temperature ionic liquid sol–gel matrix for amperometric biosensor application. *Green Chem.* **2005**, *7*, 655–658. [[CrossRef](#)]
29. Liu, Y.; Wang, M.; Li, J.; Li, Z.; He, P.; Liu, H.; Li, J. Highly active horseradish peroxidase immobilized in 1-butyl-3-methylimidazolium tetrafluoroborate room-temperature ionic liquid based sol–gel host materials. *Chem. Commun.* **2005**, 1778–1780. [[CrossRef](#)] [[PubMed](#)]
30. Shchipunov, Y.A.; Karpenko, T.Y.; Bakunina, I.Y.; Burtseva, Y.V.; Zvyagintseva, T.N. A new precursor for the immobilization of enzymes inside sol–gel-derived hybrid silica nanocomposites containing polysaccharides. *J. Biochem. Biophys. Methods* **2004**, *58*, 25–38. [[CrossRef](#)]

31. Ghorbanizamani, F.; Timur, S. Ionic Liquids from Biocompatibility and Electrochemical Aspects toward Applying in Biosensing Devices. *Anal. Chem.* **2017**, *90*, 640–648. [[CrossRef](#)]
32. Noor, S.A.M.; Bayley, P.; Forsyth, M.; MacFarlane, D. Ionogels based on ionic liquids as potential highly conductive solid state electrolytes. *Electrochim. Acta* **2012**, *91*, 219–226. [[CrossRef](#)]
33. Meyer, M.; Fischer, A.; Hoffmann, H. Novel Ringing Silica Gels That Do Not Shrink. *J. Phys. Chem. B* **2002**, *106*, 1528–1533. [[CrossRef](#)]
34. Sharp, K.G. A two-component, non-aqueous route to silica gel. *J. Sol-Gel Sci. Technol.* **1994**, *2*, 35–41. [[CrossRef](#)]
35. Néouze, M.-A.; Le Bideau, J.; Leroux, F.; Vioux, A. A route to heat resistant solid membranes with performances of liquid electrolytes. *Chem. Commun.* **2005**, 1082–1084. [[CrossRef](#)] [[PubMed](#)]
36. Néouze, M.-A.; Le Bideau, J.; Gaveau, P.; Bellayer, S.; Vioux, A. Ionogels, New Materials Arising from the Confinement of Ionic Liquids within Silica-Derived Networks. *Chem. Mater.* **2006**, *18*, 3931–3936. [[CrossRef](#)]
37. Carvalho, R.N.L. Design of Ionic Liquid-Based Biomaterials for Development of a New Generation of Biofuel Cells. Ph.D. Thesis, Instituto Superior Técnico, Universidade de Lisboa, Lisbon, Portugal, 2017.
38. Huang, X.; Brazel, C.S. On the importance and mechanisms of burst release in matrix-controlled drug delivery systems. *J. Control. Release* **2001**, *73*, 121–136. [[CrossRef](#)]
39. Stealey, S.; Khachani, M.; Zustiak, S.P. Adsorption and Sustained Delivery of Small Molecules from Nanosilicate Hydrogel Composites. *Pharmaceuticals* **2022**, *15*, 56. [[CrossRef](#)]
40. Weissig, V.; Pettinger, T.K.; Murdock, N. Nanopharmaceuticals (part 1): Products on the market. *Int. J. Nanomed.* **2014**, *9*, 4357–4373. [[CrossRef](#)]
41. Wilczewska, A.Z.; Niemirowicz, K.; Markiewicz, K.H.; Car, H. Nanoparticles as drug delivery systems. *Pharmacol. Rep.* **2012**, *64*, 1020–1037. [[CrossRef](#)]
42. Owens, G.J.; Singh, R.K.; Foroutan, F.; Alqaysi, M.; Han, C.-M.; Mahapatra, C.; Kim, H.-W.; Knowles, J.C. Sol-gel based materials for biomedical applications. *Prog. Mater. Sci.* **2016**, *77*, 1–79. [[CrossRef](#)]
43. Sankoh, S.; Vagin, M.Y.; Sekretaryova, A.N.; Thavarungkul, P.; Kanatharana, P.; Mak, W.C. Colloid electrochemistry of conducting polymer: Towards potential-induced in-situ drug release. *Electrochim. Acta* **2017**, *228*, 407–412. [[CrossRef](#)]
44. Bott, A.W.; Jackson, B.P. Study of Ferricyanide by Cyclic Voltammetry Using the CV-50W. *Curr. Sep.* **1996**, *15*, 25–30.
45. Feeney, R. Determination of heterogeneous electron transfer rate constants at microfabricated iridium electrodes. *Electrochem. Commun.* **1999**, *1*, 453–458. [[CrossRef](#)]
46. Lyons, M.E.G.; Keeley, G.P. The Redox Behaviour of Randomly Dispersed Single Walled Carbon Nanotubes both in the Absence and in the Presence of Adsorbed Glucose Oxidase. *Sensors* **2006**, *6*, 1791–1826. [[CrossRef](#)]
47. Lourenço, N.M.; Österreicher, J.A.; Vidinha, P.; Barreiros, S.; Afonso, C.A.M.; Cabral, J.M.; Fonseca, L.P. Effect of gelatin-ionic liquid functional polymers on glucose oxidase and horseradish peroxidase kinetics. *React. Funct. Polym.* **2011**, *71*, 489–495. [[CrossRef](#)]
48. Greenspan, L. Humidity fixed points of binary saturated aqueous solutions. *J. Res. Natl. Bur. Stand. A Phys. Chem.* **1977**, *81A*, 89–96. [[CrossRef](#)]
49. Zanello, P. *Inorganic Electrochemistry: Theory, Practice and Application*; Royal Society of Chemistry: London, UK, 2007. [[CrossRef](#)]
50. Carvalho, T.; Vidinha, P.; Vieira, B.R.; Li, R.W.C.; Gruber, J. Ion Jelly: A novel sensing material for gas sensors and electronic noses. *J. Mater. Chem. C* **2013**, *2*, 696–700. [[CrossRef](#)]
51. Nazet, A.; Sokolov, S.; Sonnleitner, T.; Makino, T.; Kanakubo, M.; Buchner, R. Densities, Viscosities and Conductivities of the Imidazolium Ionic Liquids [Emim][Ac], [Emim][FAP], [Bmim][BETI], [Bmim][FSI], [Hmim][TFSI], and [Omim][TFSI]. *J. Chem. Eng. Data* **2015**, *60*, 2400–2411, Correction to *J. Chem. Eng. Data* **2015**, *61*, 699–699. [[CrossRef](#)]
52. Lavagnini, I.; Antiochia, R.; Magno, F. An Extended Method for the Practical Evaluation of the Standard Rate Constant from Cyclic Voltammetric Data. *Electroanalysis* **2004**, *16*, 505–506. [[CrossRef](#)]
53. Neghmouche, N.S.; Lanez, T. Calculation of Diffusion Coefficients and Layer Thickness for Oxidation the Ferrocene using Voltammetry Technique. *Int. J. Chem. Stud.* **2013**, *1*, 28–32.
54. Bard, A.J.; Faulkner, L.R. *Electrochemical Methods: Fundamentals and Applications*, 2nd ed; Wiley: New York, NY, USA, 2001.
55. Li, W.; Tan, C.; Lowe, M.A.; Abruña, H.D.; Ralph, D.C. Electrochemistry of Individual Monolayer Graphene Sheets. *ACS Nano* **2011**, *5*, 2264–2270. [[CrossRef](#)] [[PubMed](#)]
56. Uçar, M.; Solak, A.O.; Aksu, M.; Levent, M.T. Electrochemical Investigation of 4'-Haloderivatives of N,N-Dimethyl-4-Aminoazobenzene. *Turk. J. Chem.* **2002**, *26*, 509–520.
57. Lesniewski, A.; Niedziolka, J.; Palys, B.; Rizzi, C.; Gaillon, L.; Opallo, M. Electrode modified with ionic liquid covalently bonded to silicate matrix for accumulation of electroactive anions. *Electrochem. Commun.* **2007**, *9*, 2580–2584. [[CrossRef](#)]
58. Niedziolka-Jonsson, J.; Jonsson-Niedziolka, M.; Nogala, W.; Palys, B. Electrosynthesis of thin sol-gel films at a three-phase junction. *Electrochim. Acta* **2011**, *56*, 3311–3316. [[CrossRef](#)]
59. Nicholson, R.S. Theory and Application of Cyclic Voltammetry for Measurement of Electrode Reaction Kinetics. *Anal. Chem.* **1965**, *37*, 1351–1355. [[CrossRef](#)]
60. Daum, P.H.; Enke, C.G. Electrochemical kinetics of the ferri-ferrocyanide couple on platinum. *Anal. Chem.* **1969**, *41*, 653–656. [[CrossRef](#)]

61. Gonçalves, M.C. Sol-gel Silica Nanoparticles in Medicine: A Natural Choice. Design, Synthesis and Products. *Molecules* **2018**, *23*, 2021. [[CrossRef](#)]
62. Sercombe, L.; Veerati, T.; Moheimani, F.; Wu, S.Y.; Sood, A.K.; Hua, S. Advances and Challenges of Liposome Assisted Drug Delivery. *Front. Pharmacol.* **2015**, *6*, 286. [[CrossRef](#)]